2009 American Control Conference
Hyatt Regency Riverfront, St. Louis, MO, USA
June 10-12, 2009

Rapidly Convergent Leader-Enabled Multi-Agent Deployment Into Planar Curves

Paul Frihauf and Miroslav Krstic

Abstract— **We introduce an approach for stable deployment of agents into planar curves (1-D formations in 2-D space) parameterized by the agent index. Stability is ensured by *leader* feedback, which is designed in a manner similar to boundary control of PDEs. By discretizing the model and the PDE controllers with respect to the continuous agent index, we obtain control laws for the discrete follower agents and the leader agent. The class of PDEs that motivates our design is the reaction-advection-diffusion class (broader than the standard heat equation, which is stable and does not necessitate leader feedback), which allows a much broader family of deployment profiles. Many of these profiles, however, are open-loop unstable. We stabilize them with leader feedback.**

I. Introduction

We study the problem of stabilizing planar multi-agent formations by using a leader agent to control the deployment profile and convergence rate of follower agents in each dimension independently. The deployment formations correspond to the potentially unstable, nonzero equilibria of two decoupled linear reaction-advection-diffusion PDEs. We achieve exponential stabilization of these profiles for agents modeled with single-integrator dynamics.

Research in formation control of multi-agent systems has included leaderless and leader-follower systems. In [1], feasible geometric patterns were characterized for a group of anonymous/homogeneous agents executing the same algorithm. Exponential convergence to any specified geometric pattern was proved for leaderless unicycles with a common sense of direction in [2], and convergence to generalized regular polygons was shown for unicycles under cyclic pursuit in [3]. The latter result was extended by rotating the line of sight between a pursuer and its leading neighbor to enable convergence to a point or a spiral in [4]. In [5], formation-keeping nonlinear control laws were derived for agents that follow a leader whose motion plan is generated externally. Artificial potentials and virtual leaders are used to control the group geometry and direct its mission in [6]. In related works, leader-to-formation stability was studied in [7], and the controllability of leader-follower systems is characterized in [8], [9], and [10].

Our control design utilizes the boundary control synthesis for continuous linear reaction-advection-diffusion PDEs with dynamic boundary conditions. The two boundary control laws are executed by the *leader agent* and another agent that we refer to as the *anchor agent*. In [11], the Laplacian (consensus) control, analyzed in [12], [13], and [14], was shown to coincide with the heat equation, making our model a natural extension. Continuous PDE models have been previously used to model discrete phenomena such as traffic flow [15] and the manufacture of semiconductor chips [16].

We use the 1-D backstepping approach [17] to exponentially stabilize two independent 1-D deployment profiles parameterized by the agent index, one for the horizontal coordinate and one for the vertical coordinate. This allows us to form curves in 2-D. The stabilizing PDE controllers, which are given through a continuous agent index, are then discretized to recover an ODE system that governs the dynamics of the agents. We illustrate our results with numerical simulations.

II. Leader-Enabled Deployment

For fully actuated agents in 2-D, the deployment problem consists of two decoupled 1-D deployment problems (for the horizontal and for the vertical coordinates of the agents). For this reason, we focus on 1-D deployment designs in the next four sections, only to return to 2-D applications in the simulation section (Sec. VI).

It is common to consider the heat equation

$$u_t(x,t) = u_{xx}(x,t) \tag{1}$$

as a model that governs the position $u(x,t)$ at time t of an agent indexed by x in a large (continuum) group of agents, where each agent is applying nearest-neighbor-based diffusion feedback actuated through a velocity input, namely, $v(x,t) = u_{xx}(x,t)$. This simple agent strategy is known to be stable, but it is limited in the convergence rate and is capable of achieving only linear/homogeneous (in x) deployment/equilibrium profiles (because the equilibrium equation is the simplest second order ODE, $\bar{u}''(x) = 0$).

We consider a situation where the agents are governed in each coordinate axis by a more general linear reaction-advection-diffusion equation,

$$u_t(x,t) = u_{xx}(x,t) + bu_x(x,t) + \lambda u(x,t), \quad x \in [0,1]\,, \tag{2}$$

i.e., where the velocity-actuated feedback laws of the agents are

$$v(x,t) = u_{xx}(x,t) + bu_x(x,t) + \lambda u(x,t)\,, \tag{3}$$

which are still based only on the nearest-neighbor information and where all the agents apply the same constant gains b and λ. In the sequel, we drop the arguments (x,t) whenever the context allows us to do so without harming clarity.

This work was supported by a NDSEG fellowship.

The authors are with the Department of Mechanical and Aerospace Engineering, University of California, San Diego, La Jolla, CA 92093 USA pfrihauf@ucsd.edu

With the continuum of agents being indexed from $x = 0$ to $x = 1$, we designate a special role for the two boundary agents, whose motion is governed by

$$u_t(0,t) = U_0(t), \tag{4}$$
$$u_t(1,t) = U_1(t), \tag{5}$$

where $U_0(t)$, $U_1(t)$ are controls to be designed, and which play the roles of the boundary conditions for the PDE (2).

The *leader* agent ($x = 1$) and the *anchor* agent ($x = 0$) will control the follower agents ($0 < x < 1$). As indicated by their names, the leader stabilizes the deployment profile $\bar{u}(x)$ while the anchor autonomously deploys to its designated position $\bar{u}(0)$, holding its end of the profile fixed.

The deployment profiles of interest are the nonzero equilibrium profiles of (2), which satisfy the two-point boundary value problem,

$$\bar{u}''(x) + b\bar{u}'(x) + \lambda\bar{u}(x) = 0, \tag{6}$$

with $\bar{u}(0)$ and $\bar{u}(1)$ given. This allows for a much more general family of deployment profiles than the linear (in x) equilibrium profiles of the heat equation (1). However, it is crucial to note that the equilibria described by (6) may be open-loop unstable since the eigenvalues of (2) are $\lambda - b^2/4 - \pi^2 n^2$ where $n \in \{0, 1, 2, \ldots\}$. Hence, the leader and the anchor agents will play a crucial role of stabilizing the possibly nonlinear (in x) deployment profiles.

Equation (6), which is a second-order ODE with constant coefficients, characterizes all the achievable deployment profiles with the follower agent feedbacks (3). It is of interest to see how rich the family of possible deployment profiles is. Table I categorizes the deployment profiles and their associated basis functions according to the values of b and λ. From the two decoupled PDE models, we have two deployment profiles, $\bar{u}(x)$ and $\bar{v}(x)$, that characterize a planar curve parameterized in x in the (u, v) plane,

$$u = \bar{u}(x), \quad v = \bar{v}(x), \quad x \in [0, 1]. \tag{7}$$

To the user, who has particular shapes of deployment formations in mind, these basis functions are a starting point in selecting the strategies of the follower agents, and also of the leader and anchor agents.

In this paper we present a design procedure for leader-enabled, possibly inhomogeneous, multi-agent deployment, where the user applies the following steps for both the horizontal and vertical coordinates of the agents:

1) Select the family of desired *deployment profiles*.
2) Select the *family of basis functions* that span the desired family of deployment profiles.
3) Select the *specific basis functions* by choosing the values of the advection (b) and reaction (λ) coefficients.
4) Pick *basis function coefficients* a_0 and a_1 to generate the specific deployment profile $\bar{u}(x)$.
5) Pick the desired deployment *convergence rate*.
6) Discretize the continuous model (2), (4), (5) spatially to obtain implementable control laws for the leader, anchor, and follower agents.

TABLE I

1-D DEPLOYMENT PROFILES OF THE REACTION-ADVECTION-DIFFUSION EQUATION.

b, λ	**1-D Deployment Profile** $\bar{u}(x)$	**Basis Functions**
$b = \lambda = 0$	$a_0 + a_1 x$	$(1, x)$
$b \neq 0$, $\lambda = 0$	$a_0 + a_1 e^{-bx}$	$\left(1, e^{-bx}\right)$
$b = 0$, $\lambda > 0$	$a_0 \cos(\theta x) + a_1 \sin(\theta x)$, $\theta = \sqrt{\lambda}$	$(\cos(\theta x), \sin(\theta x))$
$b^2 = 4\lambda$	$(a_0 + a_1 x)\, e^{-\sigma x}$, $\sigma = \sqrt{\lambda}$	$\left(e^{-\sigma x}, x e^{-\sigma x}\right)$
$b^2 < 4\lambda$	$e^{\sigma x}\,(a_0 \cos(\theta x) + a_1 \sin(\theta x))$, $\sigma = -\frac{b}{2}$, $\theta = \frac{1}{2}\sqrt{4\lambda - b^2}$	$(e^{\sigma x}\cos(\theta x)$, $e^{\sigma x}\sin(\theta x))$
$b^2 > 4\lambda$	$a_0 e^{\sigma_0 x} + a_1 e^{\sigma_1 x}$, $\sigma_{0,1} = -\frac{b}{2} \pm \frac{1}{2}\sqrt{b^2 - 4\lambda}$	$(e^{\sigma_0 x}, e^{\sigma_1 x})$

The key to this procedure is a step that is not included in this list, as it is not a routine user step. This is the step of designing the control laws for the anchor/leader inputs $U_0(t)$, $U_1(t)$ appearing in (4), (5). We now focus on the design of these control laws.

III. LEADER FEEDBACK DESIGN

We employ PDE backstepping boundary control [17]. First, we introduce the deployment profile error,

$$z(x,t) = u(x,t) - \bar{u}(x), \tag{8}$$

to shift the equilibrium to the origin. Substituting (8) into (2), (4), and (5), yields

$$z_t = z_{xx} + bz_x + \lambda z, \tag{9}$$
$$z_t(0) = Z_0(t), \tag{10}$$
$$z_t(1) = Z_1(t), \tag{11}$$

where $Z_0(t) = U_0(t)$ and $Z_1(t) = U_1(t)$. Next, we eliminate the advection term by using the change of variable,

$$v(x) = z(x)e^{\frac{b}{2}x}, \tag{12}$$

as shown in [17]. Substituting (12) into (9)–(11) results in the reaction-diffusion equation

$$v_t = v_{xx} + \left(\lambda - \frac{b^2}{4}\right) v, \tag{13}$$
$$v_t(0) = V_0(t), \tag{14}$$
$$v_t(1) = V_1(t), \tag{15}$$

where $V_0(t) = Z_0(t)$ and $V_1(t) = e^{\frac{b}{2}} Z_1(t)$.

Let $w(x,t)$ be a new state that is defined by the coordinate transformation [17],

$$w(x,t) = v(x,t) - \int_0^x k(x,y)v(y,t)\,dy\,. \tag{16}$$

where the kernel $k(x,y)$ defined on $\mathcal{T} = \{(x,y) : 0 \leq y \leq x \leq 1\}$ is given by

$$k(x,y) = -\bar{c}y\frac{I_1\left(\sqrt{\bar{c}\,(x^2 - y^2)}\right)}{\sqrt{\bar{c}\,(x^2 - y^2)}}, \tag{17}$$

$\bar{c} = c + \lambda - b^2/4$, and I_1 denotes the first order modified Bessel function of the first kind.

Remark 3.1: The transformation (16) can be inverted to obtain

$$v(x,t) = w(x,t) + \int_0^x l(x,y)w(y,t)\,dy, \tag{18}$$

where the inverse gain kernel $l \in \mathcal{C}^2(\mathcal{T})$ [17].

The variable (16) is shown to satisfy the target system

$$w_t = w_{xx} - cw - k_y(x,0)w(0), \tag{19}$$

$$w_t(0) = -cw(0), \tag{20}$$

$$w_t(1) = -cw(1), \tag{21}$$

where $c > 0$. From (12), (16), and (20),

$$Z_0(t) = -cz(0), \tag{22}$$

is immediate, and from (8) and (22), we obtain the anchor's control law,

$$U_0(t) = -c\left(u(0) - \bar{u}(0)\right). \tag{23}$$

To define the leader's control law, we introduce the operator $\mathcal{K}\{\cdot\}$ acting on a function $\xi(x,t)$ as

$$\begin{aligned}\mathcal{K}\{\xi\}(t) = &-\sqrt{\bar{c}}\,I_1\left(\sqrt{\bar{c}}\right)e^{-\frac{b}{2}}\xi(0,t)\\ &-\left(\frac{\bar{c}^2}{8} + \frac{b\bar{c}}{4} - \frac{\bar{c}}{2} + c\right)\xi(1,t) - \frac{\bar{c}}{2}\xi_x(1,t)\\ &-\int_0^1 e^{-\frac{b}{2}(1-y)}\left(\bar{c}y^3\frac{I_3\left(\sqrt{\bar{c}\,(1-y^2)}\right)}{\left(\bar{c}\,(1-y^2)\right)^{\frac{3}{2}}}\right.\\ &-3y\frac{I_2\left(\sqrt{\bar{c}\,(1-y^2)}\right)}{\bar{c}\,(1-y^2)}\\ &\left.+\,y\frac{I_1\left(\sqrt{\bar{c}\,(1-y^2)}\right)}{\sqrt{\bar{c}\,(1-y^2)}}\right)\bar{c}^2\xi(y,t)\,dy,\end{aligned} \tag{24}$$

where I_2 and I_3 indicate the second and third order modified Bessel functions of the first kind respectively. From (12), (16), and (21), we find

$$Z_1(t) = \mathcal{K}\{z\}(t). \tag{25}$$

Then from (8) and (25), we arrive at the leader's control law,

$$U_1(t) = \mathcal{K}\{u\}(t) - \mathcal{K}\{\bar{u}\}, \tag{26}$$

that, with (23), stabilizes the deployment profile $\bar{u}(x)$.

Of note, the control laws (23) and (26) both contain a feedback term and a constant bias term. These bias terms can be computed prior to deployment according to the desired deployment profile. Thus, by simply changing the bias—without changing the feedback—different deployment profiles can be stabilized. When the bias terms are zero, rendezvous at the origin is achieved.

IV. Closed-Loop Stability

There are several aspects in which the stability analysis here differs from that in [17]. This is due to the dynamic character of the boundary conditions (20), (21), which require that the analysis be conducted in the space H^1 rather then L^2, and due to the additional (perturbation) term on the right-hand side of (19).

Theorem 1: The system (2) with boundary conditions (4), (5) and control laws (23), (26) is exponentially stable in the H^1 norm at the equilibrium $u(x,t) \equiv \bar{u}(x)$, i.e., there exists $M > 0$ such that for all $t > 0$,

$$\Omega(t) \le Me^{-ct}\Omega(0), \tag{27}$$

where

$$\Omega(t) = z(0,t)^2 + z(1,t)^2 + \|z(t)\|_{L^2}^2 + \|z_x(t)\|_{L^2}^2, \tag{28}$$

$c > 0$, and $c \neq \frac{b^2}{4} - \lambda$.

Proof: Let $V(t)$ be the Lyapunov functional

$$\begin{aligned}V(t) = &\frac{m_0}{2}w(0,t)^2 + \frac{1}{2}w(1,t)^2\\ &+ \frac{m_1}{2}\|w(t)\|_{L^2}^2 + \frac{1}{2}\|w_x(t)\|_{L^2}^2,\end{aligned} \tag{29}$$

where m_0 and m_1 are positive scalars to be determined. In the sequel, we omit the arguments (x,t) unless needed for clarity.

Computing the time derivative of $V(t)$ and substituting (19)–(21) yields

$$\begin{aligned}\dot{V} = &-cm_0w(0)^2 - cw(1)^2 - cm_1\int_0^1 w^2\,dx\\ &- m_1w(0)\int_0^1 k_y(x,0)w\,dx + m_1\int_0^1 ww_{xx}\,dx\\ &+ \int_0^1 w_xw_{xt}\,dx.\end{aligned} \tag{30}$$

Integrating by parts the last two terms of (30), gives

$$\begin{aligned}\dot{V} = &-cm_0w(0)^2 - cw(1)^2 + m_1ww_x|_0^1 + w_xw_t|_0^1\\ &- cm_1\int_0^1 w^2\,dx - m_1\int_0^1 w_x^2\,dx\\ &- m_1w(0)\int_0^1 k_y(x,0)w\,dx - \int_0^1 w_{xx}w_t\,dx.\end{aligned} \tag{31}$$

Again we substitute (19)–(21) and collect terms to obtain

$$\begin{aligned}\dot{V} = &-cm_0w(0)^2 - cw(1)^2 + (m_1 - c)\,ww_x|_0^1\\ &- cm_1\int_0^1 w^2\,dx - m_1\int_0^1 w_x^2\,dx - \int_0^1 w_{xx}^2\,dx\\ &- w(0)\int_0^1 k_y(x,0)\left(m_1w - w_{xx}\right)\,dx + c\int_0^1 ww_{xx}\,dx.\end{aligned} \tag{32}$$

Integrate the last term in (32) by parts to get

$$\begin{aligned}\dot{V} \leq & -cm_0 w(0)^2 - cw(1)^2 + m_1 w w_x|_0^1 \\ & - cm_1 \int_0^1 w^2\,dx - (m_1+c)\int_0^1 w_x^2\,dx - \int_0^1 w_{xx}^2\,dx \\ & + |w(0)|\left|\int_0^1 k_y(x,0)\,(m_1 w - w_{xx})\,dx\right|. \end{aligned} \tag{33}$$

We now apply the Cauchy-Schwarz Inequality and Young's Inequality to obtain

$$\begin{aligned}\dot{V} \leq & -cm_0 w(0)^2 - cw(1)^2 + m_1 w w_x|_0^1 \\ & - cm_1 \int_0^1 w^2\,dx - (m_1+c)\int_0^1 w_x^2\,dx \\ & - \int_0^1 w_{xx}^2\,dx + \frac{1}{2}w(0)^2\int_0^1 k_y(x,0)^2\,dx \\ & + \frac{1}{2}\int_0^1 \left(m_1^2 w^2 - 2m_1 w w_{xx} + w_{xx}^2\right)\,dx. \end{aligned} \tag{34}$$

Integrating the last term of (34) by parts gives

$$\begin{aligned}\dot{V}(t) \leq & -\left(c - \frac{1}{2m_0}\int_0^1 k_y(x,0)^2\,dx\right) m_0 w(0,t)^2 \\ & - cw(1,t)^2 - \left(c - \frac{m_1}{2}\right) m_1 \int_0^1 w(x,t)^2\,dx \\ & - c\int_0^1 w_x(x,t)^2\,dx - \frac{1}{2}\int_0^1 w_{xx}(x,t)^2\,dx, \\ \leq & -\min\left(c - \frac{\Lambda}{2m_0}, c - \frac{m_1}{2}\right)\left(m_0 w(0,t)^2\right. \\ & \left. + w(1,t)^2 + m_1\|w(t)\|_{L^2}^2 + \|w_x(t)\|_{L^2}^2\right), \end{aligned} \tag{35}$$

where

$$\begin{aligned}\Lambda &= \int_0^1 k_y(x,0)^2\,dx, \\ &= \frac{2}{3}\bar{c}^2\, I_0\left(\sqrt{\bar{c}}\right)^2 - \frac{2}{3}\bar{c}\sqrt{\bar{c}}\, I_0\left(\sqrt{\bar{c}}\right) I_1\left(\sqrt{\bar{c}}\right) \\ &\quad - \frac{1}{3}\bar{c}\, I_1\left(\sqrt{\bar{c}}\right) - \frac{2}{3}\bar{c}^2\, I_1\left(\sqrt{\bar{c}}\right)^2. \end{aligned} \tag{36}$$

We select $m_0 = \Lambda/c$ and $m_1 = c$ to obtain

$$\dot{V} \leq -cV. \tag{37}$$

(The choice of m_0 assumes that $c \neq \frac{b^2}{4} - \lambda$ so that $\Lambda > 0$.)

By the Comparison Lemma,

$$V(t) \leq e^{-ct}V(0). \tag{38}$$

From Lemma 1 and (38), we have

$$\begin{aligned}\Omega(t) &\leq \frac{1}{p_1}\Psi(t) \leq \frac{1}{p_1 q_1}V(t) \leq \frac{1}{p_1 q_1}e^{-ct}V(0), \\ &\leq \frac{q_2}{p_1 q_1}e^{-ct}\Psi(0) \leq \frac{p_2 q_2}{p_1 q_1}e^{-ct}\Omega(0), \end{aligned} \tag{39}$$

where $q_1 = \frac{1}{2}\min\left(1, \frac{\Lambda}{c}, c\right)$, $q_2 = \frac{1}{2}\max\left(1, \frac{\Lambda}{c}, c\right)$, and p_1 and p_2 are shown in (53). The result (27) is obtained from (39) with $M = \frac{p_2 q_2}{p_1 q_1}$. ■

V. Discretized Agent Control Laws

To move from a continuum of agents to a model for a finite number, we spatially discretize the continuous model (2) and the leader agent's feedback (26). The anchor agent's control law (23) does not require any modification since it depends only on the anchor agent's position. The state variable $u(x,t)$ becomes $u(ih,t)$ where $i = 0,\ldots,n+1$, $h = 1/(n+1)$, and n is the number of follower agents. We denote the leader agent as u_{n+1}, the anchor agent as u_0, and the follower agents as u_i.

For the leader agent, we define the operator $\mathcal{K}_D\{\cdot\}$, a discretized version of (24), acting on a function $\xi(ih,t)$, as

$$\begin{aligned}\mathcal{K}_D\{\xi\}(t) = & -\sqrt{\bar{c}}\, I_1\left(\sqrt{\bar{c}}\right) e^{-\frac{b}{2}}\xi_0(t) \\ & - \left(\frac{\bar{c}^2}{8} + \frac{b\bar{c}}{4} - \frac{\bar{c}}{2} + c\right)\xi_{n+1}(t) \\ & - \frac{\bar{c}}{2}\left(\frac{\xi_{n+1}(t) - \xi_n(t)}{h}\right) \\ & - \frac{h}{2}\left(f_{n+1}(t) + 2\sum_{i=1}^{n} f_i(t)\right), \end{aligned} \tag{40}$$

where

$$\begin{aligned}f_i(t) = e^{-\frac{b}{2}(1-ih)}\Bigg(& \bar{c}(ih)^3 \frac{I_3\left(\sqrt{\bar{c}\,(1-(ih)^2)}\right)}{\left(\bar{c}\,(1-(ih)^2)\right)^{\frac{3}{2}}} \\ & - 3ih\frac{I_2\left(\sqrt{\bar{c}\,(1-(ih)^2)}\right)}{\bar{c}\,(1-(ih)^2)} \\ & + ih\frac{I_1\left(\sqrt{\bar{c}\,(1-(ih)^2)}\right)}{\sqrt{\bar{c}\,(1-(ih)^2)}}\Bigg)\bar{c}^2\xi_i(t), \end{aligned} \tag{41}$$

$$f_{n+1}(t) = \frac{\bar{c}^2}{48}\left(\bar{c}+6\right)\xi_{n+1}(t). \tag{42}$$

To obtain (40), we use the trapezoidal rule and the two-point backward difference to approximate the integral term and the $u_x(1)$ term in (24). With (40), the leader's discretized control law is simply,

$$U_{n+1}(t) = \mathcal{K}_D\{u\}(t) - \mathcal{K}_D\{\bar{u}\}. \tag{43}$$

We discretize the follower agent control laws (2) by using three-point central differencing to approximate the spatial derivatives and by averaging the reaction term, obtaining

$$\begin{aligned}U_i(t) = & \frac{u_{i+1} - 2u_i + u_{i-1}}{h^2} + b\frac{u_{i+1} - u_{i-1}}{2h} \\ & + \lambda\left(pu_{i-1} + (1-2p)u_i + pu_{i+1}\right), \end{aligned} \tag{44}$$

where p is a positive scalar to be determined. Together, the control laws (23), (43), and (44) govern the dynamics of the agents according to the ODE system,

$$\dot{u}_0 = U_0(t), \tag{45}$$

$$\dot{u}_i = U_i(t), \tag{46}$$

$$\dot{u}_{n+1} = U_{n+1}(t). \tag{47}$$

The approximation error of (43) and (44) due to the spatial discretization increases as the discretization becomes coarser

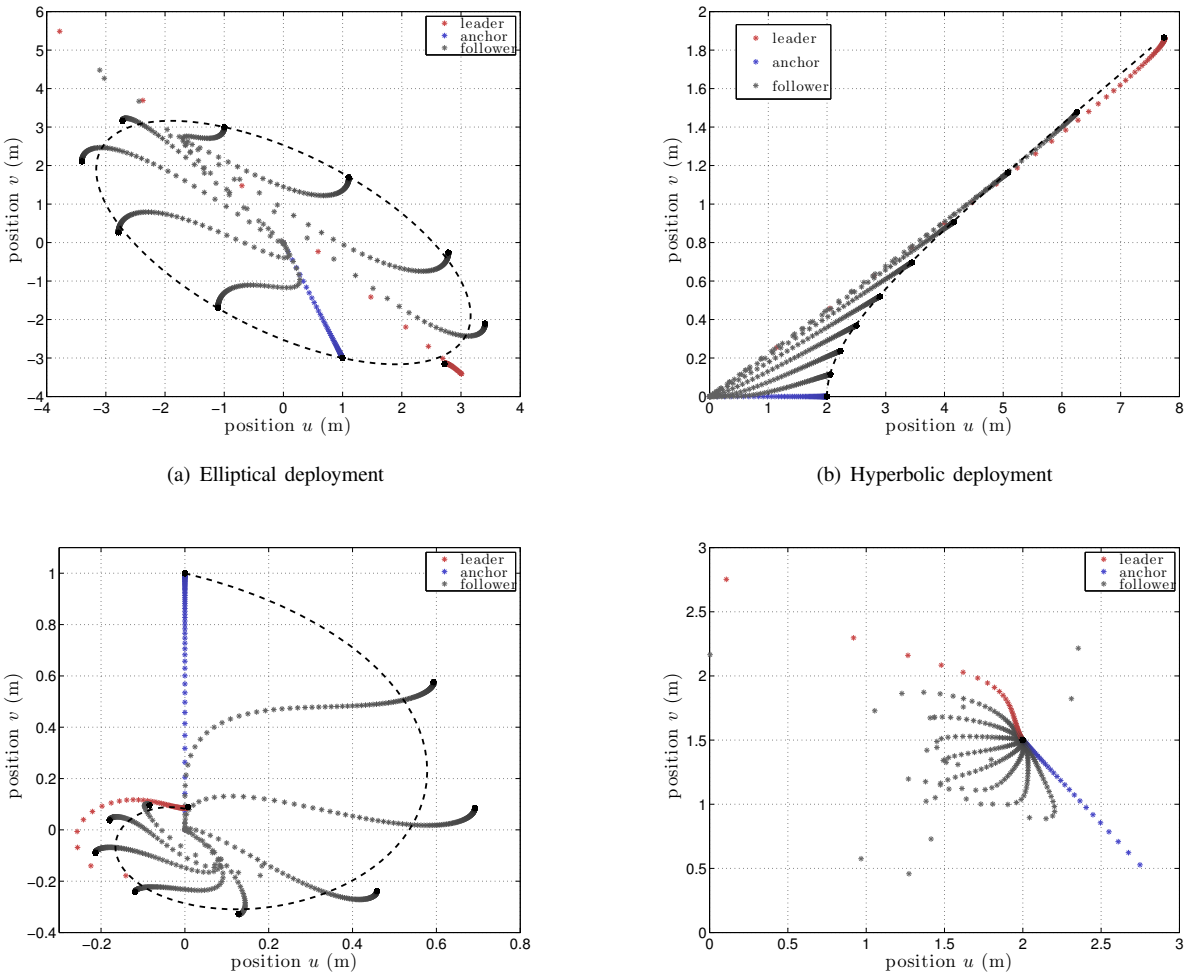

(a) Elliptical deployment

(b) Hyperbolic deployment

(c) Circular logarithmic spiral deployment

(d) Rendezvous at $(2, 1.5)$

Fig. 1. Agent trajectories for deployments (a)-(c) with agents initialized at the origin and rendezvous (d) with agents initialized from a random uniform distribution. Darker shading indicates advances in time where $t \in [0, 2]$ sec.

(fewer agents are deployed). Consequently, the equilibria of (45)–(47) start to significantly deviate from the desired deployment profiles in Table I for small numbers of agents. We use p as a tool to force the equilibria to match the nonzero equilibrium profiles of (2) in a least squares sense.

We determine p by assuming that the equilibrium $\bar{u}_i$, which satisfies $\dot{u}_i(t) = 0$, is equal to the deployment profile $\bar{u}(ih)$, leaving p as the only unknown variable. We obtain the over-determined system of equations, $Ap = B$, where

$$A = \lambda h^2 \begin{pmatrix} \bar{u}_0 - 2\bar{u}_1 + \bar{u}_2 \\ \bar{u}_{i-1} - 2\bar{u}_i + \bar{u}_{i+1} \\ \bar{u}_{n-1} - 2\bar{u}_n + \bar{u}_{n+1} \end{pmatrix}, \tag{48}$$

$$B = \begin{pmatrix} \alpha\bar{u}_0 + \left(2 - \lambda h^2\right)\bar{u}_1 - \beta\bar{u}_2 \\ \alpha\bar{u}_{i-1} + \left(2 - \lambda h^2\right)\bar{u}_i - \beta\bar{u}_{i+1} \\ \alpha\bar{u}_{n-1} + \left(2 - \lambda h^2\right)\bar{u}_n - \beta\bar{u}_{n+1} \end{pmatrix}, \tag{49}$$

$$\alpha = \frac{bh}{2} - 1, \quad \beta = 1 + \frac{bh}{2}, \quad i = 1, \ldots, n, \tag{50}$$

and solve for p using the pseudo-inverse of A.

We see directly from (43) and (44) that the spatial discretization imposes a fixed communication topology where the follower agents depend only on their nearest neighbors, and the leader requires global information to stabilize the deployment. Such a topology is not uncommon in leader-follower systems when the leader is responsible for controlling the behavior of the follower agents.

VI. Simulations

We simulate ten agents ($n = 8$) in the (u, v) plane by implementing the control laws (23), (43), and (44) to stabilize decoupled 1-D deployments along each axis. In this manner, we achieve 2-D planar curves parameterized in x.

For example, we stabilize the ellipse (Fig. 1(a)), $\left(\frac{3u+v}{8}\right)^2 + \left(\frac{u+3v}{8}\right)^2 = 1$, and the hyperbola (Fig. 1(b)), $(u/2)^2 - (2v)^2 = 1$, using the parameter sets $(b = 0, \lambda = 4\pi^2(\frac{n+1}{n+2})^2, c = 10, p = 0.0850)$ and $(b = 0, \lambda = -4, c = 10, p = 0.0831)$. In Fig. 1(c), we stabilize a circular logarithmic spiral, $u = e^{-\frac{5}{2}x}\sin(2\pi x)$, $\quad v = e^{-\frac{5}{2}x}\cos(2\pi x)$, where $x \in [0, 1]$, which corresponds to $b = 5$ and $\lambda =$

$4\pi^2 + 25/4$. The gain $c = 25$ and $c = 15$ was used when stabilizing the u- and v-axis deployment profiles with $p = 0.1128$.

Our final example uses control laws derived from the heat equation (1) to enable the agents to rendezvous at a selected point. Fig. 1(d) shows the agents rendezvousing at the point $(2, 1.5)$ after being initialized randomly from a uniform distribution. The parameter $c = 10$ was used. One should note that the leader does not simply move directly to the rendezvous point, but instead takes a route that influences the followers and speeds convergence.

VII. Conclusions

We have introduced a PDE boundary control-based approach for stable leader-enabled deployment of 2-D formations of agents. While the standard diffusion-based feedback for individual agents leads to inherently stable deployment into equidistant profiles, for which leader assistance is not needed, the non-equidistant profiles that we pursue here may be open-loop unstable. In our approach, the leader feedback stabilizes such profiles.

The approach that we present here is based on reaction-advection-diffusion PDEs and allows stable deployment into profiles where the agent displacement can be represented by the following functions of the agent index: linear (standard), $\sin, \cos, \sinh, \cosh, \exp$. This allows deployment formations of practical interest—for example, the leader deploying out the majority of agents near a target position (occupied by the anchor agent) while staying at base and keeping very few agents near base, or conversely, deploying out only a few agents; deploying agents out in both directions symmetrically while both the leader and anchor stay at base, thus creating a "protective shell" for the leader; or deploying the agents to encircle a point of interest.

It is crucial to observe that in our leader-enabled framework the follower agents deploy out not by being commanded some reference positions, but by being induced (indirectly influenced) by the leader's and anchor's motions to deploy out and to maintain a stable formation.

Future work includes stabilizing formations with observer-based feedback and modeling the agents with nonholonomic vehicle dynamics. Additionally, nonlinear PDE models will further broaden the types of formations that can be stabilized.

References

[1] I. Suzuki and M. Yamashita, "Distributed anonymous mobile robots: formation of geometric patterns." *SIAM Journal on Computing*, vol. 28, no. 4, pp. 1347–1363, 1999.

[2] Z. Lin, B. Francis, and M. Maggiore, "Necessary and sufficient graphical conditions for formation control of unicycles." *IEEE Transactions on Automatic Control*, vol. 50, no. 1, pp. 121–127, 2005.

[3] J. A. Marshall, M. E. Broucke, and B. A. Francis, "Formations of vehicles in cyclic pursuit." *IEEE Transactions on Automatic Control*, vol. 49, no. 11, pp. 1963–1974, 2004.

[4] M. Pavone and E. Frazzoli, "Decentralized policies for geometric pattern formation and path coverage." *Journal of Dynamic Systems, Measurement, and Control*, vol. 129, pp. 633–643, Sept 2007.

[5] J. P. Desai, J. Ostrowski, and V. Kumar, "Controlling formations of multiple mobile robots." *Robotics and Automation*, vol. 4, pp. 2864–2869, 1998.

[6] N. Leonard and E. Fiorelli, "Virtual leaders, artificial potentials and coordinated control of groups." *IEEE Conference on Decision and Control*, vol. 3, pp. 2968–2973, 2001.

[7] H. Tanner, G. Pappas, and V. Kumar, "Leader-to-formation stability." *IEEE Trans. Robotics and Automation*, vol. 20, no. 3, pp. 443–455, 2004.

[8] M. Ji and M. Egerstedt, "A graph-theoretic characterization of controllability for multi-agent systems." *American Control Conference*, pp. 4588–4593, 2007.

[9] B. Liu, T. Chu, L. Wang, and G. Xie, "Controllability of a leader-follower dynamic network with switching topology." *IEEE Transactions on Automatic Control*, vol. 53, no. 4, pp. 1009–1013, 2008.

[10] A. Rahmani and M. Mesbahi, "Pulling the strings on agreement: anchoring, controllability, and graph automorphisms." *American Control Conference*, pp. 2738–2743, 2007.

[11] G. Ferrari-Trecate, A. Buffa, and M. Gati, "Analysis of coordination in multi-agent systems through partial difference equations," *IEEE Transactions on Automatic Control*, vol. 51, no. 11, pp. 918–928, 2006.

[12] A. Jadbabaie, J. Lin, and A. S. Morse, "Coordination of groups of mobile autonomous agents using nearest neighbor rules." *IEEE Transactions on Automatic Control*, vol. 48, no. 6, pp. 988–1001, 2003.

[13] L. Moreau, "Stability of continuous-time distributed consensus algorithms." *IEEE Conference on Decision and Control* pp. 3998–4003, 2004.

[14] R. Olfati-Saber and R. M. Murray, "Consensus problems in networks of agents with switching topology and time-delays." *IEEE Transactions on Automatic Control*, vol. 49, no. 9, pp. 1520–1533, 2004.

[15] M. J. Lighthill and G. B. Whitham, "On kinematic waves II. A theory of traffic flow on long crowded roads." *Proceedings of the Royal Society of London. Series A, Mathematical and Physical Sciences (1934-1990)*, vol. 229, no. 1178, pp. 317–345, 1955.

[16] D. Armbruster, C. Ringhofer, and T.-C. Jo, "Continuous models for production flows." *American Control Conference*, vol. 5, pp. 4589–4594, 2004.

[17] A. Smyshlyaev and M. Krstic, "Closed-form boundary state feedbacks for a class of 1-D partial integro-differential equations," *IEEE Transactions on Automatic Control*, vol. 49, pp. 2185–2204, 2004.

[18] M. Krstic and A. Smyshlyaev, *Boundary Control of PDEs: A Course on Backstepping Designs*, 1st edition, SIAM, Philadelphia, PA, 2008.

Appendix

Lemma 1: There exists p_1, p_2, q_1, $q_2 > 0$ such that

$$p_1\Omega(t) \le \Psi(t) \le p_2\Omega(t), \tag{51}$$

$$q_1\Psi(t) \le V(t) \le q_2\Psi(t), \tag{52}$$

where $\Psi(t) = w(0,t)^2 + w(1,t)^2 + \|w(t)\|^2_{L^2} + \|w_x(t)\|^2_{L^2}$, and $\Omega(t)$ and $V(t)$ are shown in (28) and (29).

Proof: Using (12), (16), and (18), one can obtain

$$p_1 = \frac{1}{l_1 n_1}, \quad p_2 = l_2 n_2, \tag{53}$$

where

$$l_1 = \max\left(2 + b^2 + (12 + b^2)L + 8L_x, 4\right), \tag{54}$$

$$l_2 = \max\left(2 + b^2 + 8K + 4K_x, 4\right), \tag{55}$$

$$L = \sup_{(x,y)\in\mathcal{T}} |l(x,y)|^2, \tag{56}$$

$$L_x = \sup_{(x,y)\in\mathcal{T}} |l_x(x,y)|^2, \tag{57}$$

$$K = \sup_{(x,y)\in\mathcal{T}} |k(x,y)|^2, \tag{58}$$

$$K_x = \sup_{(x,y)\in\mathcal{T}} |k_x(x,y)|^2, \tag{59}$$

$n_1 = \max\left(1, e^{-b}\right)$, and $n_2 = \max\left(1, e^{b}\right)$, to satisfy (51).

With $q_1 = \frac{1}{2}\min(1, m_0, m_1)$ and $q_2 = \frac{1}{2}\max(1, m_0, m_1)$, equation (52) is immediate. ∎